Short Communication

Atomic Identification of Fluorescent Q-Dots on Tau-Positive Fibrils in 3D-Reconstructed Pick Bodies

Miho Uematsu,*[†] Eijiro Adachi,*[‡]
Ayako Nakamura,* Kuniaki Tsuchiya,[§] and
Toshiki Uchihara*

From the Laboratory of Structural Neuropathology,* Tokyo Metropolitan Institute of Medical Science, Tokyo; the Department of Neurology,[†] Tokyo Metropolitan Neurological Hospital, Tokyo; the Department of Matrix Biology and Tissue Regeneration,[‡] Kitasato University Graduate School of Medical Sciences, Kanagawa; and the Department of Laboratory Medicine and Pathology,[§] Tokyo Metropolitan Matsuzawa Hospital, Tokyo, Japan

Pick body disease, characterized by the presence of Pick bodies, is distinguished from neurofibrillary tangles in Alzheimer disease on the basis of their smooth, spherical shape. Quantum dots (QDs) are nanometer-scale, water-soluble fluorophores that are detectable both as a fluorescent signal by light microscopy and as electron-dense particles under electron microscopy. In this study, tau-positive Pick bodies were immunofluorescently labeled with QD nanocrystals composed of cadmium selenide for three-dimensional (3D) reconstruction and subsequently subjected to electron microscopic observation to identify QD immunolabeling on the same Pick body for comparison in detail. The identity of the QD nanocrystals, which label the tau-positive fibrils, was confirmed by the presence of both cadmium and selenium on these nanocrystals, demonstrated as parallel peaks corresponding to these atoms on energy-dispersive X-ray spot analysis under super-resolution scanning transmission electron microscopy. This confirmation of the specificity of the QD labeling through both its fluorescence and energy-dispersive X-ray spectra reinforces the reliability of the labeling. In addition, this exact comparison of the same structure by electron microscopy and 3D light microscopy demonstrates how its ultrastructural details are related to its surrounding structures on a 3D basis, providing further insights into how molecules woven into specific pathological ultrastructures are at work *in situ*. *(Am J Pathol 2012, 180: 1394–1397; DOI: 10.1016/j.ajpath.2011.12.029)

Pick body disease is pathologically characterized by the presence of Pick bodies (PBs), defined initially as "eine dunkle argentophile Kugel" (a dark, argentophilic sphere) by Alois Alzheimer.[1] From the beginning, Alzheimer distinguished PBs from neurofibrillary tangles on the basis of their smooth spherical shape occasionally containing lacunae inside. It is now established that typical PBs are composed of three-repeat tau woven into straight hollow filaments of 15 nm in diameter arranged in random directions.[2,3] However, their three-dimensional (3D) structure at light microscopy (LM) level and their exact relation to ultrastructural details still remain speculative because direct comparison between 3D structure and its ultrastructure was not readily possible.

Quantum dots (QDs) are nanometer-scale water-soluble fluorophores composed typically of cadmium selenide clusters comprising the core with a zinc sulfide shell.[4] Labeling by QDs is detectable both as fluorescent signal at LM[4] and as electron-dense particles with characteristic halo under electron microscopy (EM).[5] By taking advantage of this dual property of QDs as a probe, it is possible to observe the same target in two ways after QD labeling, first through their fluorescence at LM, followed by EM to detect electron-dense particles of QD. Although this correlative light/electron microscopy method[6] has been so far successful on thin histological sections, we recently expanded this strategy on a 3D basis to compare the fluorescent profile of a target point of axonal α-synuclein (αS) and its exact EM findings (3D-oriented immunoEM).[7] Because the staining profile of axonal αS is heterogeneous from one point to another,

accurate identification of the point of interest for comparison to bridge LM and EM findings is essential. In the present study, this 3D-oriented immunoEM is applied to PBs, which is further combined with an energy-dispersive X-ray (EDX) analysis to confirm that the labeling by the electron-dense particles contain Se and Zn, major constituents of QDs.

Materials and Methods

Tissue Preparation

We studied three autopsied brain tissue samples of sporadic cases of Pick body disease with clinical history of progressive dementia, aphasia, personality change, and extrapyramidal symptoms. The neuropathological diagnosis of Pick body disease was based on the frontotemporal atrophy and the presence of PBs.[8] Formalin-fixed tissue blocks of the temporal lobe were washed in 0.1 mol/L phosphate buffer and cryoprotected with 15% sucrose/phosphate buffer overnight at 4°C and then in 30% sucrose/phosphate buffer for a week. The tissue was frozen at or around −10°C in OCT compound and cut into 50-μm-thick floating sections on a freezing microtome.

Immunohistochemistry

The sections were washed with 0.01 mol/L phosphate-buffered saline (PBS), blocked for 30 minutes in 5% normal goat serum/PBS, and incubated in mouse anti-phosphorylated tau monoclonal antibody (AT8; Innogenetics, Zwijndrecht, Belgium) diluted to 1:500 in PBS/0.05% normal goat serum at 4°C for more than a week. Because the fluorescent signal from QDs is less intense than conventional fluorochromes, this primary antibody (AT8) was initially labeled with Alexa Fluor 546 conjugated with an anti-mouse IgG made in goat (Molecular Probes, Eugene, OR), diluted 1:200 in PBS for 2 hours in the dark, to facilitate identification and 3D reconstruction. This secondary antibody (goat IgG) was subsequently labeled with an anti-goat IgG antibody conjugated with QD 655 (Invitrogen, Carlsbad, CA) diluted to 1:100 in 0.05% bovine serum albumin (BSA) for 5 hours in the dark. Sections were washed in 0.05% BSA in PBS. After washing in PBS, the sections were mounted with buffered glycerol containing *p*-phenylenediamine.

Fluorescent Confocal Microscopic Observation

Among the three cases, which similarly exhibited intense AT8 fluorescence signals on PBs, sections containing the cells of interest with PBs were selected and observed under a fluorescence microscope equipped with a laser confocal system (Leica TCS/SP5, Heidelberg, Germany) using a ×40 oil immersion objective lens. Alexa 546 was excited using a green helium-neon laser (543 nm), and the detection bandwidth was set at 570 to 615 nm (expected peak at 573 nm). QD 655–antibody conjugate was excited with an argon laser (488 nm), and the detection bandwidth was set at 640 to 685 nm so that its

emission peak at 655 nm was included whereas the signal from Alexa 546 was excluded. Z-series scan (41.0 × 41.0 μm:512 × 512 pixels) with an interval of 0.07 μm was performed, and the data were processed on public-domain image analysis software ImageJ64 (NIH, Bethesda, MD), and volume-rendered 3D images were reconstructed using a 3D projection program and plug-in 3D viewer. For example, a series of 300 optical slices (20-μm thick in total) were necessary to encompass the entire PB and the neuron harboring this PB as a whole.

Identification of the Same Pick Body for Electron Microscopic Observation

After making the recording for the 3D reconstruction, the exact same neuron containing the PB was identified with an inverted fluorescence microscope equipped with UV laser Micro Dissection System PALM MB-III (P.A.L.M. Microlaser Technologies, Bernried, Germany). Holes were punched by a UV laser as landmarks around this target neuron containing the PB, with the Alexa 546 signal as a guide. The same section was then detached from the glass slide and fixed in 2% glutaraldehyde, postfixed in 1% osmium tetroxide, and embedded in epon. The Epon-embedded block was trimmed so that the target neuron containing the same PB, already digitally reconstructed as a 3D data set, was identified using the punched-out holes as landmarks for orientation.[7] Ultrathin sections including the target neuron were stained with uranyl acetate and examined with an electron microscope H-7650 (Hitachi High-Technologies, Tokyo, Japan).

EDX Analysis of QD Nanoparticles

Hitachi HD-2000 scanning transmission electron microscope (STEM) was operated at 200 kV in this study. The STEM is equipped with a cold-field emission gun and detectors that consist of bright-field, high-angle annular dark-field (HAADF), and secondary electron (SE) detectors for observation. This instrument is also equipped with an EDX Si(Li) detector (EDAX Genesis system, Osaka, Japan) with a collection angle of 0.3 sr and an X-ray take-off angle of 25°, and X-ray signals were acquired. Bright-field and HADDF-STEM images with 1280 × 960 pixels were acquired with an incident beam of 0.5 nm for a frame time of 40 seconds per image. EDX point analyses were performed with an incident beam size of 0.5 nm and a current of 0.1 nA. The acquisition time of the single point was 2 minutes.

Results

Observation under the confocal laser scanning microscope showed numerous AT8-positive PBs, most frequently in the granule cell layer of the dentate gyrus of the hippocampus and less frequently in the parahippocampal gyrus and temporal cortex. Although the signal from QD655 (Figure 1, A and B) was less intense than that from Alexa546 (Figure 1, C–E), both fluorochromes pro-
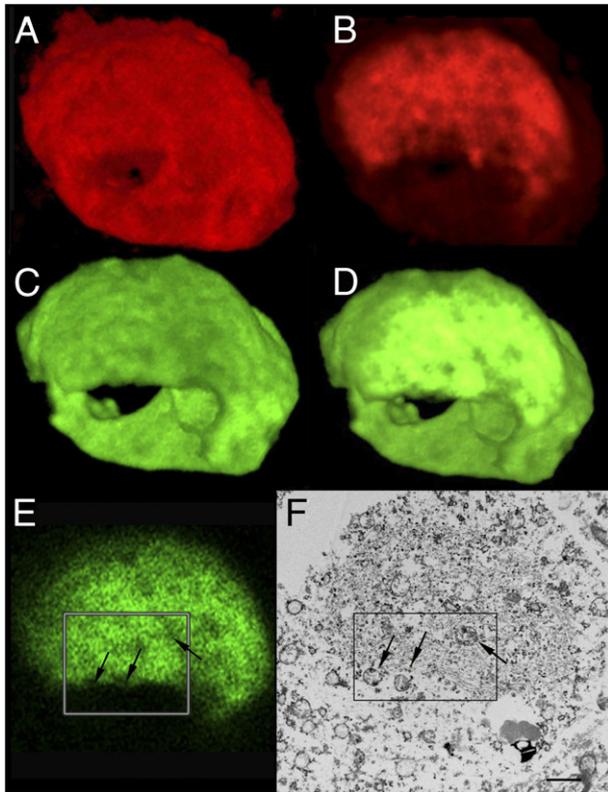
Figure 1. Three-dimensional reconstruction of a PB and its optical slice and corresponding to ultrathin section for electron microscopy. AT8-positive material in a PB in a thick floating section labeled by QD655 (red) and Alexa 546 (green) was observed under the confocal microscope to obtain Z-stack images. They were volume-rendered into 3D images (**A** and **C**). **B** and **D:** Images show the cut surface of a PB sectioned at the level that is shown in **E**. After obtaining the data set for 3D reconstruction (**A–D**), the same floating section was prepared for electron microscopic observation (**F**). Its corresponding optical section, retrieved from the 3D data set, is shown (**E**). The **rectangles** indicate the corresponding area between **E** and **F**. Tau-negative lacunae in the PB (**arrows**, **E**) are identified as mitochondria on EM (**arrows** in **F**). Scale bar = 1 μm.

plasmic reticulum, and the lysosomes, and their clusters (PBs) are not surrounded by limiting membrane. These electron-dense particles are rod-shaped with a halo, a morphological signature compatible with QD655 (Figure 2C. Furthermore, EDX spot analysis demonstrated two parallel peaks representing Se and Cd exclusively on these particles (Figure 2, C-E), whereas these peaks were not evident on fibrils without these particles (Figure 2, C and F) and on background (Figure 2, C and G), which confirmed the identity of these electron-dense particles on fibrils as QD.

Discussion

Some degenerative lesions in the human brain are characterized by progressive aggregation of multiple proteins to form representative 3D complexes as a signature of

vided essentially identical images after reconstruction in three dimensions. Although PBs are known to be round, 3D reconstruction demonstrated a variety of PBs of heterogeneous morphologies that may be oval, parachute-like, worm- or doughnut-shaped, and others. They were often eccentrically located at the periphery of a neuron and were facing each other with nuclei. They frequently contained several tau-negative lacunae inside (see Supplemental Video S1 at *http://ajp.amjpathol.org*). Similar results were obtained on vibratome sections from the same cases (data not shown).

Figure 1E represents an optical plane retrospectively retrieved from the 3D data set of the PB, which exactly corresponds to its Epon-embedded counterpart at low-power magnification on EM (Figure 1F). Notably, not only the external contour of this PB, but also its internal details (Figure 1, E and F) are exactly comparable between the fluorescence slice (Figure 1E) and its Epon-embedded counterpart (Figure 1F). A close-up view (Figure 2A) of the target area (Figure 1F) demonstrates randomly oriented fibrils 15 nm in diameter labeled by abundant electron-dense particles (Figure 2, B and C). These fibrils had no spatial relationship with Golgi apparatus, the endo-

Figure 2. Higher magnifications of a PB immunolabeled by QD655, confirmed by energy-dispersive X-ray analysis. Panel A corresponds to the **rectangle** shown in Figure 1, E and F. **Arrows** indicate the identical mitochondria as seen in Figure 1F. **B:** A higher magnification of the **rectangle** in **A**. **C:** Higher magnification of the **rectangle** in **B**. **D–G:** EDX spectra at the points indicated by **arrowheads** in **C**. **D** and **E:** QD655 on the fibers, where combined peaks corresponding to Se and Cd are confirmed as specific constituents of QD655. These peaks were absent on the fiber without QD655 (**F**) and background (**G**) 200-kV high-angle annular dark-field STEM mode. Scale bars: 0.5 μm (**A**); 100 nm (**B**); and 50 nm (**C**).

the disease process.[9] Because these lesions chronologically develop by being molded according to underlying structures, their biochemical and structural compositions are not homogeneous, and their diversity may represent some differences according to the nature and developing stage of the lesion. One of the examples is Lewy bodies, where progressive aggregation of αS, initially as pale bodies, evolves into more solid Lewy bodies,[10,11] whereas their relation to axonal aggregates remained speculative. Recently, we were successful in detecting αS-positive fibers in axons by first identifying their fluorescent profile of QDs, which labeled the target axonal aggregates, followed by EM observation of the exact same axonal aggregate, where QD labeling is detectable as electron-dense particles with a characteristic halo.[7] This direct comparison was achieved by LM detection of QD fluorescence for 3D reconstruction and subsequent preparation of the same section for EM to identify QD particles on the same target. EM orientation of the target was guided by holes punched out around the target after recording QD fluorescence for 3D reconstruction. Preprocessing Z-stack images provided referential 2D information on arbitrary sections of the target structure, making it feasible to find the LM plane exactly corresponding to the ultrathin section processed for EM. This direct comparison of LM profile and ultrastructure, which we established as "3D-oriented immunoEM,"[7] is particularly useful to pinpoint the target within a lesion to examine how its fluorescence profile is related to its ultrastructure. Although the ultrastructural identity of QDs is based on their size and surrounding halo, their electron density is much lower, and their contour is more obscure than conventional immunogold particles. In the present study, EDX spot analysis demonstrated parallel peaks corresponding to Cd and Se on the electron-dense particles, compatible with QDs on the target fibers (Figure 2, C–E), but not on fibers themselves (Figure 2, C and F) or background (Figure 2, C and G). A similar approach on immunogold particles and QDs[12] has already been reported. However, direct comparison between the LM plane corresponding to the EM section, as we established with 3D-oriented immunoEM,[7] is highly advantageous in analyzing degenerative lesions in human brains, where heterogeneous profiles are piled up to form a 3D complex. Dual demonstration of the identity of QDs, through fluorescence and EDX spot analysis, ultimately confirmed the specificity of the labeling. Although PBs are described as spherical structures in the neuronal cytoplasm,[13] our 3D analysis demonstrated that PBs are of heterogeneous morphologies and contain lacunae inside as described by Alzheimer.[1] Comparison between their fluorescent profile and ultrastructure demonstrated that AT8-positive material (Figure 1, A–E) corresponds exactly to accumulation of AT8-labeled fibers (Figures 1 and 2) in PBs. Their relation to organellae such as mitochondria or lipofuscin granules is readily recognizable in detail (Figure 1, E and F). Although routine formalin fixation of the samples used in this study hampered more detailed examination of AT8-labeled fibers and their relation to organellae, this method to observe intracytoplasmic inclusions on both LM and EM in parallel would allow a closer insight into the functions of a molecule to form the ultrastructure, and its relation to LM findings of the exact same target. This approach to examine molecular localization, both at the ultrastructural and LM levels, offers a promising method to bridge a molecule integrated in a complex structure with its functions in physiological and pathological conditions.

References

1. Alzheimer A: Über eingenartige Krankheitsfälle des spätern Alters [Concerning a unique disease of the cerebral cortex]. Zeitschr Gesam Neurol Psychiat 1911, 4:356–385
2. Delacourte A, Robitaille Y, Sergeant N, Buée L, Hof PR, Wattez A, Laroche-Cholette A, Mathieu J, Chagnon P, Gauvreau D: Specific pathological Tau protein variants characterize Pick's disease. J Neuropathol Exp Neurol 1996, 55:159–68
3. Uchihara T, Tsuchiya K: Neuropathology of Pick body disease. Dementias, ch 35. Handbook of Clinical Neurology, 3rd series, vol 89. Edited by C Duyckaerts, I Litvan. Amsterdam, Elsevier, 2008, pp. 415–430
4. Hines MA, Guyot-Sionnest P: Synthesis and characterization of strongly luminescing ZnS-capped CdSe nanocrystals. J Phys Chem 1996, 100:468–471
5. Timp W, Watson N, Sabban A, Zik O, Matsudaira P: Wet electron microscopy with quantum dots. Biotechniques 2006, 41:295–298
6. Cortese K, Diaspro A, Tacchetti C: Advanced correlative light/electron microscopy: current methods and new developments using Tokuyasu cryosections. J Histochem Cytochem 2009, 57:1103–1112
7. Kanazawa T, Adachi E, Orimo S, Nakamura A, Mizusawa H, Uchihara T: Pale neurites, premature α-synuclein aggregates with centripetal extension from axon collaterals. Brain Pathol. 2012, 22:67–78
8. McKhann GM, Albert MS, Grossman M, Miller B, Dickson D, Trojanowski JQ; Work Group on Frontotemporal Dementia and Pick's Disease: Clinical and pathological diagnosis of frontotemporal dementia: report of the Work Group on Frontotemporal Dementia and Pick's Disease. Arch Neurol 2001, 58:1803–1809
9. Uchihara T, Nakamura A, Nakayama H, Arima K, Ishizuka N, Mori H, Mizushima S: Triple immunofluorolabeling with two rabbit polyclonal antibodies and a mouse monoclonal antibody allowing three-dimensional analysis of cotton wool plaques in Alzheimer disease. J Histochem Cytochem 2003, 51:1201–1206
10. Forno LS: Neuropathology of Parkinson's disease. J Neuropathol Exp Neurol 1996, 55:259–272
11. Spillantini MG, Schmidt ML, Lee VM, Trojanowski JQ, Jakes R, Goedert M: Alpha-synuclein in Lewy bodies. Nature 1997, 388:839–840
12. Loukanov A, Kamasawa N, Danev R, Shigemoto R, Nagayama K: Immunolocalization of multiple membrane proteins on a carbon replica with STEM and EDX. Ultramicroscopy 2010, 110:366–374
13. Lowe J, Mirra SS, Hyman BT et al.: Pick's disease. Greenfield's Neuropathology, ed 8. Edited by Love S, Louis DN, Ellison DW London, Hoddler Arnold, 2008, pp 1087–1090